



STRENGTHENING BEAM-COLUMN JOINTS: EXPLORING NATURAL FIBRE REINFORCEMENT FOR ENHANCED STRUCTURAL RESILIENCE UNDER CYCLIC LOADING

Dr. Eldho N V, Jini Alias, Muhammed Thanzah K H, Abdhul Basith A

Departments: Chemistry, Electronics and Communication Engineering (ECE), Civil Engineering,
Indira Gandhi Institute of Engineering and Technology
Nellikuzhi P.O, Kothamangalam, Ernakulam (Dist), Kerala, Pincode 68669, India

Abstract

In the event of a breakdown, the joints that connect the beams and columns are the most crucial failure zones. Whenever dynamic stresses are applied to the concrete, the bonding of the rebars will be significantly strained, and it will eventually break. It is possible that the collapse of the joint point will not only cause damage to the column loading routes, but it may also have an effect on the overall ductility of the structure as well as its ability to dispense energy. The purpose of this research was to investigate the connection between natural fibre and beam-column joints by incorporating sisal fibre into reinforced concrete at fractions ranging from 0.5 percent to 1.5 percent, with an increase of 0.25%. The IS 13920-2016 was followed in order to complete the ductile details. The study is built taking into consideration the effects of cyclic loading with the help of the finite element software ANSYS workbench, which is used to carry out the analysis. A Finite Element Method (FEM) study was performed in order to investigate the behaviour of the structure when subjected to cyclic loading. This analysis included a comparison of the maximum load and displacement values with the experimental data. According to the findings of a comparison between finite element modelling (FEM) analysis and actual values, the addition of 1.25 percent sisal fibre to reinforced concrete results in improved performance at the junction between a beam and a column in terms of its ability to sustain lateral and seismic stresses on the structures.

Keywords: *Beam column joint, Sisal fiber, Cyclic loading, FEM analysis, Displacement, ANSYS.*

1. Introduction

The beam-column joints in earthquake-prone locations are often considered a critical element in reinforced concrete constructions [1, 2]. The use of closely spaced hoops as transverse reinforcement was recommended to ensure the beam-column connection had the necessary ductility [3]. Several researchers have attempted to alleviate the technical difficulties by minimising the joint reinforcement arrangement [4]. Fiber-reinforced concrete is preferred because it increases congestion and makes the consolidation of concrete in the joints more difficult [5]. Various experimental investigations have



proposed using NaturalFiberReinforcedConcrete (NFRC) as additional reinforcement instead of compressing stirrups in the beam-column joints. The beam-column assemblages of existing framed structures were traditionally designed to function with a weak column-strong beam configuration [6]. Seismic forces may cause localised hinges to form in the column. By modifying the current beam-column connections to function in a manner where the column is weaker than the beam, it becomes feasible to overcome this problem and achieve cost and time savings [7]. This repeated pattern of activity may compromise the structural integrity of the structure. The brittle structural failure serves as an indicator of the related failure mode, representing the minimum level of strength in the hierarchy and being directly linked to it [8, 9]. It stands out even more since it is the only failure mode characterised by a fragile structural collapse. One method to identify this failure is by recognising that it is associated with this specific failure mode [10, 11]. The literature has examined various techniques for repairing and strengthening weakened concrete, including epoxy repair, elimination and replacement, as well as the use of Prestressed Concrete (PC) jacketing, construction unit wrapping, partial masonry infill, steel jacketing, and addition to external steel elements. Additionally, the use of Fiber-Reinforced Polymer (FRP) materials has been studied for these purposes [12, 13]. Additional methods include using steel jacketing and incorporating external steel components. Other approaches for installation include the use of exterior steel components, masonry unit jacketing, partial masonry infill, steel jacketing, and a combination of masonry unit jacketing and steel jacketing [14, 15]. Every plan requires a certain amount of creative complexity, as well as careful consideration of personnel costs, range of application, and disruption to building occupancy [16]. According to an extensive literature study, there is a limited amount of information available on the behaviour of small-scale experiments using square RC columns covered in Glass Fibre Reinforced Polymer (GFRP) with varying corner angles. The control specimens consisted of three unwrapped columns. Each of the three columns was coated with either one or two layers of Glass Fibre Reinforced Polymer (GFRP). The angle corners of each column were covered with a 25 mm layer. The columns clad with GFRP experienced more axial movement compared to the control column in order to enhance their compressive strength [17, 18].

2. Analytical Investigation

2.1. Modelling

An ANSYS software was used to perform Finite Element Analysis (FEA) on the connection between the beam and the column under cyclic loading conditions. This was conducted to assess the response of the joint under the specified loading circumstances. The FEA study of the connection joint specimens includes both material and geometric nonlinearities. This guarantees the precision of the analysis. In a nonlinear analysis, the total specified loads applied to a body consisting of finite components will be separated into discrete load increments. This will verify that the body is able to bear the specified loads. Following each increase, the structure reaches a state of near-equilibrium, and the stiffness matrix of the structure is modified to account for any nonlinear alterations that may have taken place in the overall stiffness of the structure [19].

2.1.1. Element

In the exterior connection specimens shown in Figure 1, a consistent mesh size of 10 mm was chosen for the concrete components over the whole geometry. Steel bars are used in conjunction with reinforcing mesh of same dimensions. This design consists of 15246 pieces and 32461 nodes.

2.1.2. Loading and Boundary Condition

Figure 2 provides a comprehensive depiction of the geometry and boundary conditions of the reinforced concrete beam-column connections used in the finite element method (FEM) study. During the first phase, the upper surface of the column is uniformly exposed to a constant compressive axial load throughout the study. During the second phase, the specimen is subjected to a unidirectional lateral load applied to the end surface of the beam.

2.1.3. Specification of Materials

The concrete material characteristics utilised in the study reported in Table 1 are the compressive and tensile strengths, Poisson's ratio, and Young's modulus of elasticity (E_c). Concrete material is subjected to experimental assessments to determine its Poisson's ratio value, which is thereafter used. The steel reinforcement displayed elastic uniaxial tensile stress-strain behaviour, with a Young's modulus of 2×10^5 MPa and a Poisson's ratio of 0.28.

2.1.4. Details of reinforcement

A total of twelve specimens were created, each representing a cross section of an exterior beam-column junction. The beam span for each specimen was 1.5 metres, while the column height was 1 metre. The beams had dimensions of 200 mm width and 150 mm height, while the columns had dimensions of 150 mm width and 150 mm height. Every specimen is equipped with reinforcement detailing that conforms to the criteria set by IS456-2000, as well as detailing that complies to the specifications established by IS13920-1993. The reinforcement may be supplied in bars with diameters varying from 4 to 12 mm, and stirrups with a diameter of 8 mm, evenly spaced 120 mm apart from centre to centre. The beam and column's anchoring zones are reinforced with 8 mm stirrups for tensile strength at the connection. The distance between the stirrups varies from 75 mm to 300 mm. Figure 3 depicts the enhanced characteristics of the beam-column junction.

The experimental setup comprises a response frame, a hydraulic actuator with a power of 400kN and a stroke length of 100 mm. The frame has a load capacity of 50 KN and applies stresses to the test specimens using a hydraulic jack seen in Figure 4. Linear Variable Differential Transducers (LVDT) were used at the top of the column to measure lateral displacement. Additionally, a single load cell connected to the actuator was used to measure cyclic lateral loads.

3. Results of Finite Element Method (FEM) Analysis

Figure 5 illustrates the susceptible connections to lateral loading between reinforced concrete beams and columns. The connections are shown in Figure 5. The load-displacement curves seen at the specimen joint help to depict the Finite Element Analysis (FEA) outcomes for these connections. This is done to provide a precise representation of the findings [20-23].

4. Findings and Analysis

Table 2 presents the highest sideways forces and movements obtained from experimental tests and represented by numerical modelling. Figure 6 presents a comparison between the load-displacement curves predicted by the simulation and the experimental findings obtained from beam-column junction specimens. After using the FEA approach, the ultimate strength of CCBCJ 01 rose by 6% compared to the control specimens. Similarly, SFBCJ 0.5, SFBCJ 0.75, SFBCJ 1, SFBCJ 1.25, and SFBCJ 1.5 experienced increases of 23%, 28%, 34%, and 17% correspondingly, compared to the control specimens. A uniform increase in deflections was noted in all specimens. Based on the findings made by the finite element analysis, the behaviour of the material after it has yielded shows some deviation from its initial response, similar to the results obtained in the test [24]. This phenomenon may be attributed to some pre-existing assumptions, such as the selection of certain compressive and tensile characteristics of concrete, the intrinsic variations in the presence and alignment of fibres, and the common errors connected with experimental endeavours [25, 26].

Comparative analysis of the Damage Index in relation to the Number of Cycles

Figure 7 displays the cumulative damage index values of all test specimens obtained from the finite element analysis (FEM). A damage index for various characteristics of reinforced concrete, which is often used, was introduced in a study [27]. This index is described as a linear equation that combines the standardised maximum deflection and the normalisation hysteretic energy, as seen below.

$$D = \frac{\delta_m}{\delta_u} + \frac{\beta}{F_y \delta_u} \int dE \quad (1)$$

The symbol δ_m represents the most favourable amount of deformation resulting from seismic forces and is the optimal deformation experienced under cyclic loads. F_y represents the strength at which yielding occurs, dE represents the incremental absorption of hysteretic energy, and β represents the impact of cyclic loading on structural damage. The damage index is a standardised measure that ranges from zero to one. A D.I number of 0 shows that the structure is intact and exhibits elastic behaviour caused by an earthquake. On the other hand, a D.I value of 1 implies structural failure, meaning a complete collapse of the structure.

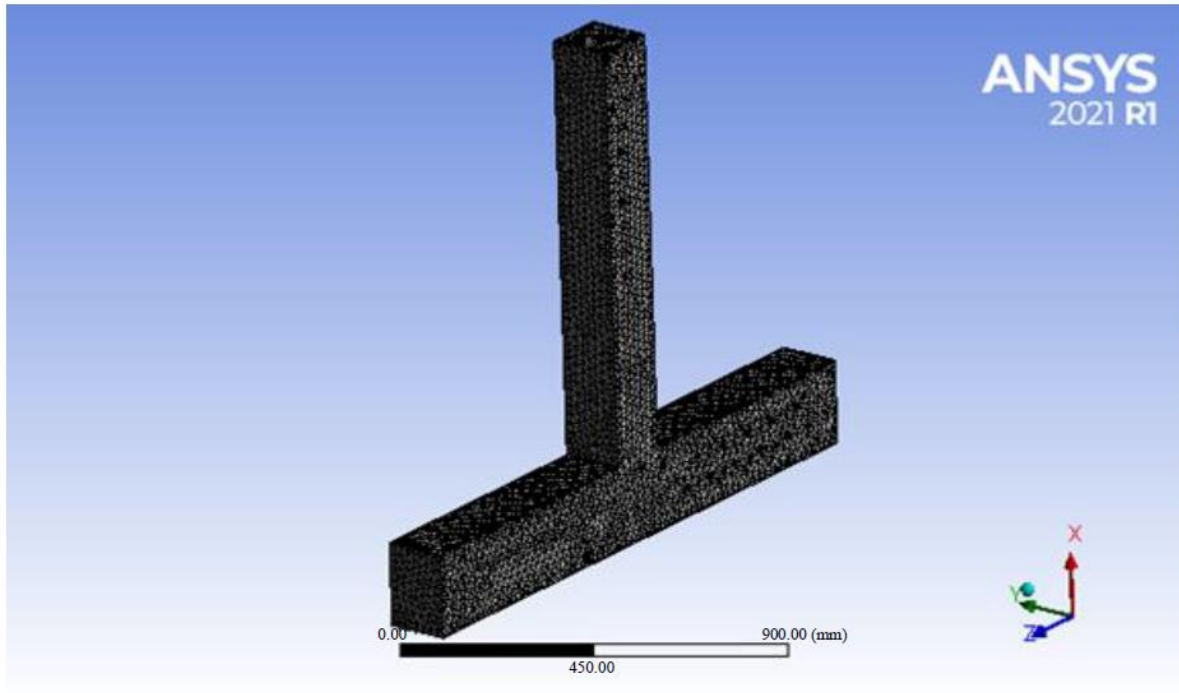


Fig. 1 Concrete element mesh of exterior connection

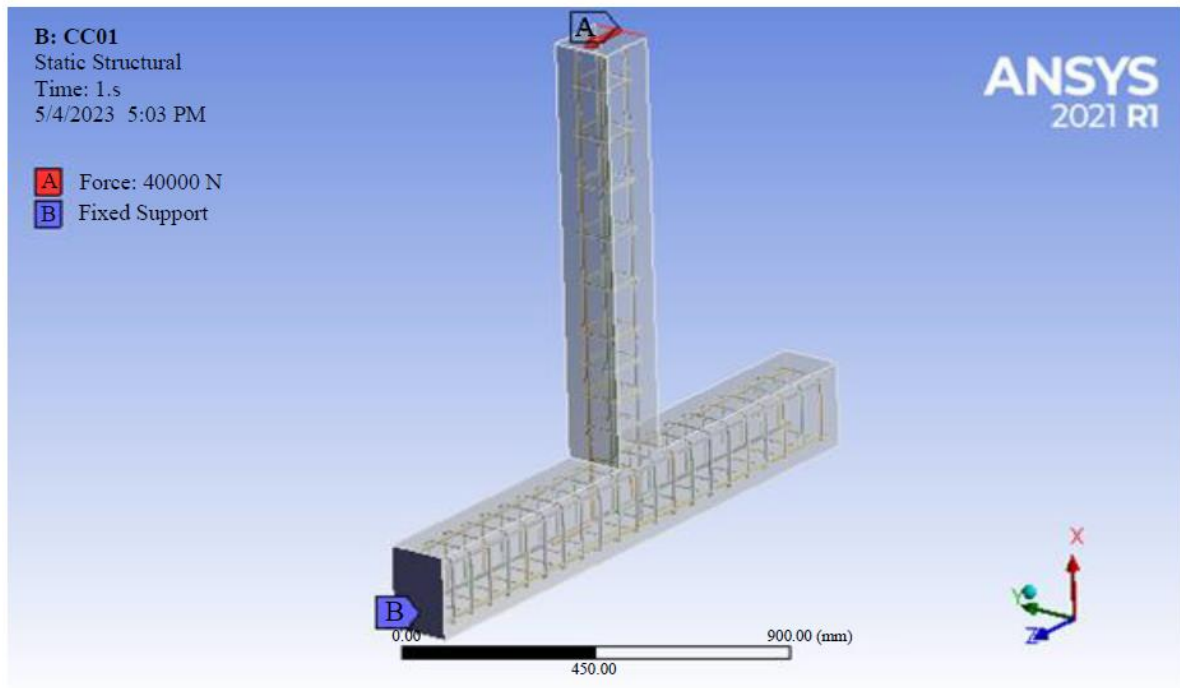


Fig. 2 Reinforcement details of the exterior connection

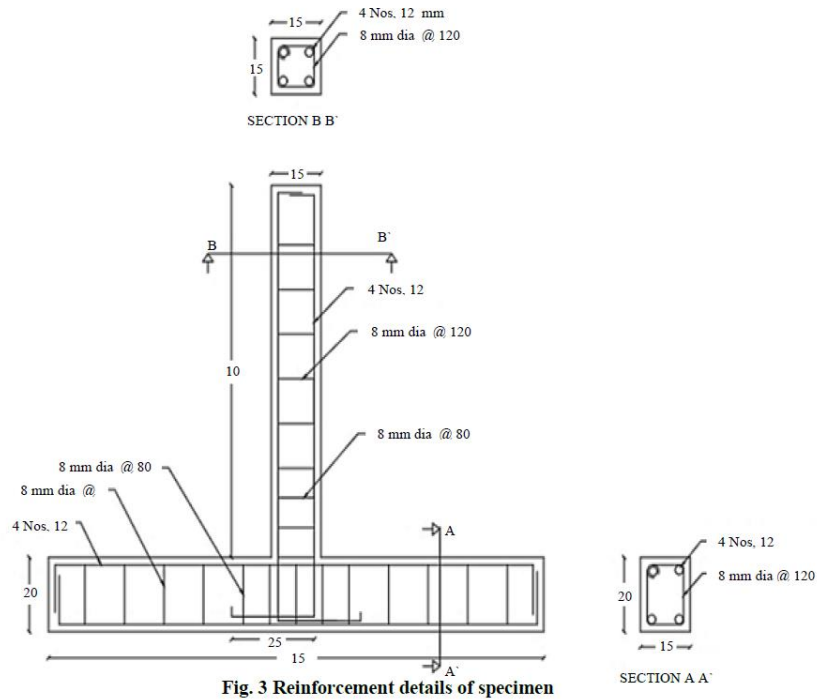
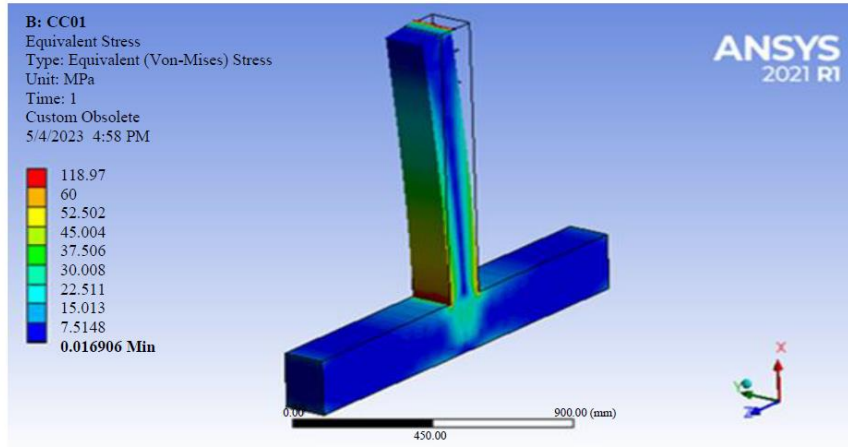


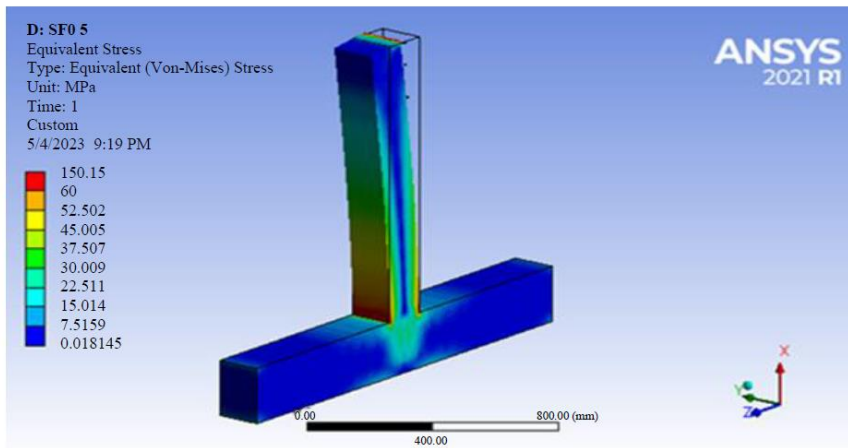
Fig. 3 Reinforcement details of specimen



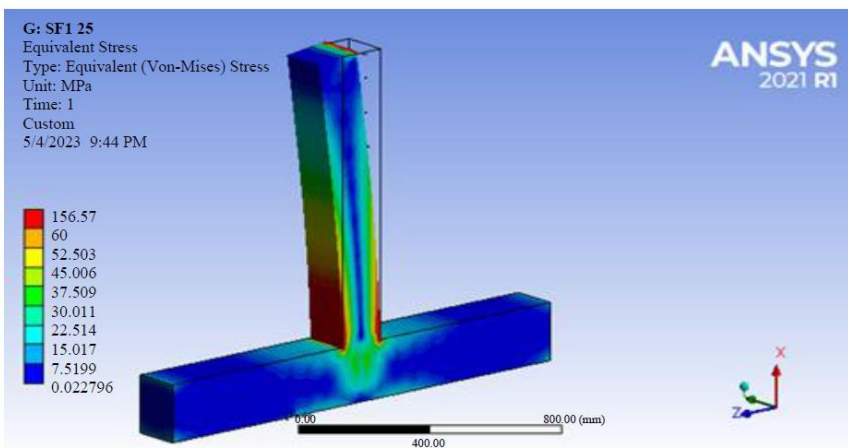
Fig. 4 Experimental setup for the beam-column joint



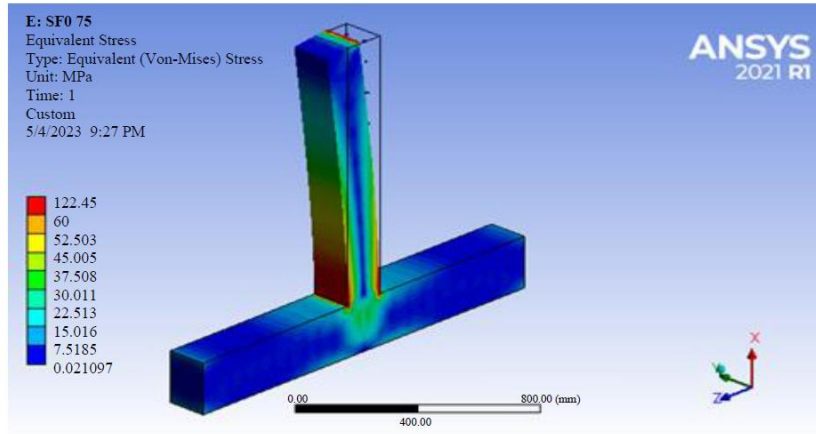
(a)



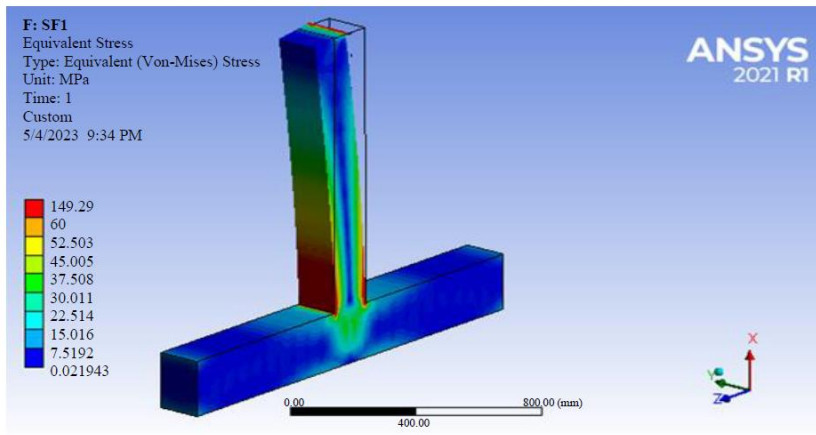
(b)



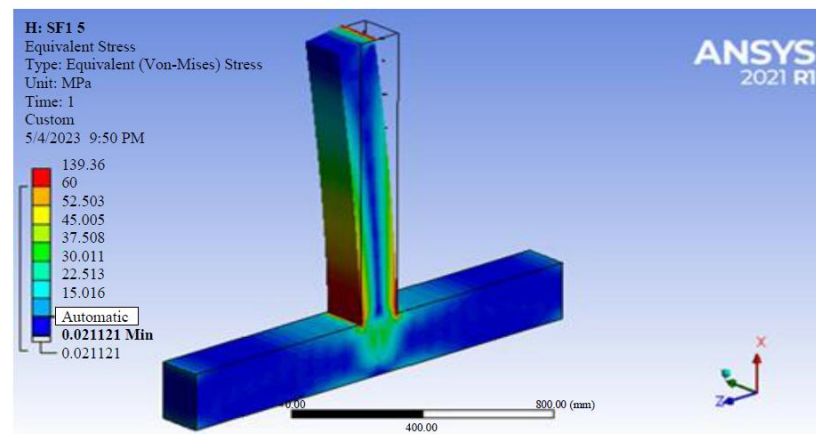
(c)



(d)

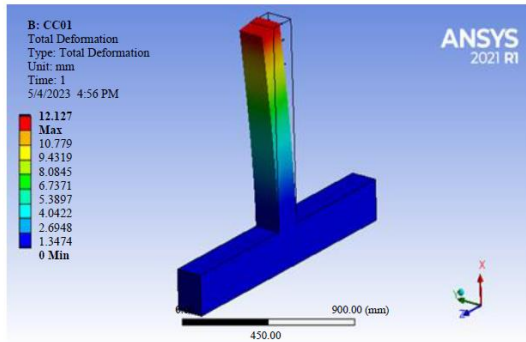


(e)

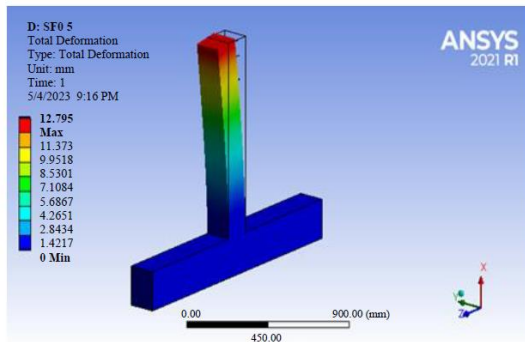
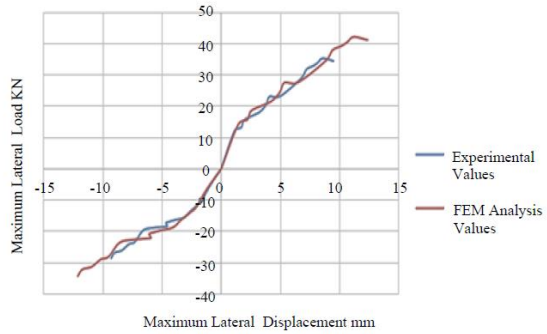


(f)

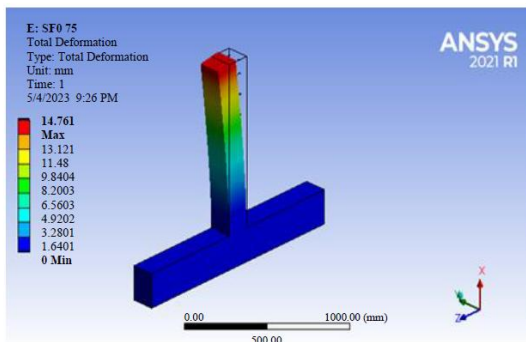
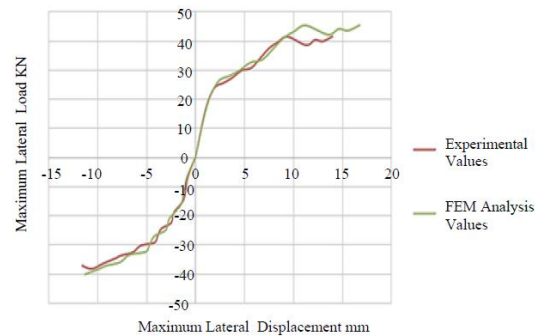
Fig. 5 (a) CCBCJ 01, (b) SFBCJ 0.5, (c) SFBCJ 0.75, (d) SFBCJ 1, (e) SFBCJ 1.25, (f) SFBCJ 1.5 Lateral load and displacement obtained from FEM



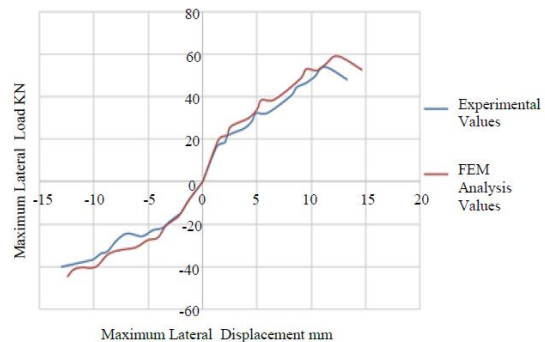
(a) Maximum displacement - CCBCJ 01

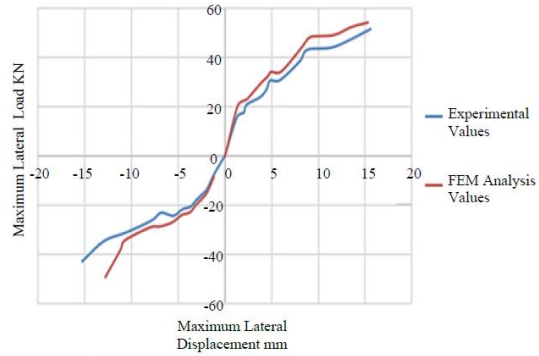
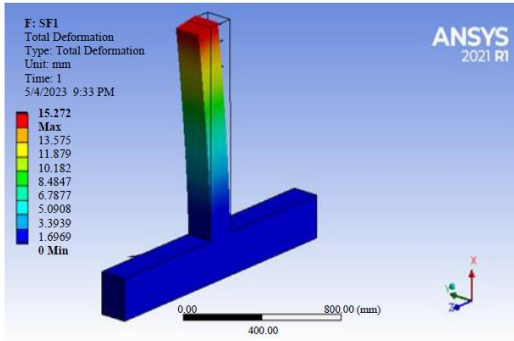


(b) Maximum displacement - SFBCJ 0.5

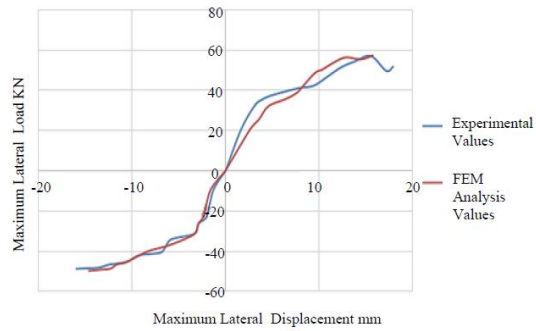
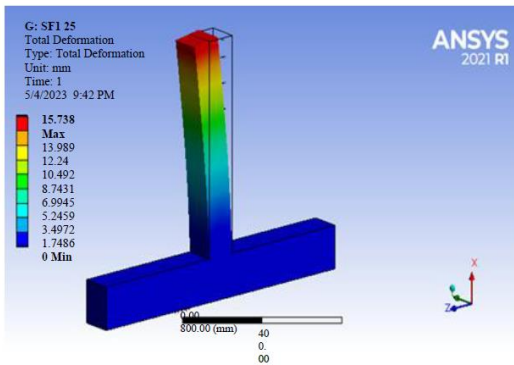


(c) Maximum displacement - SFBCJ 0.75

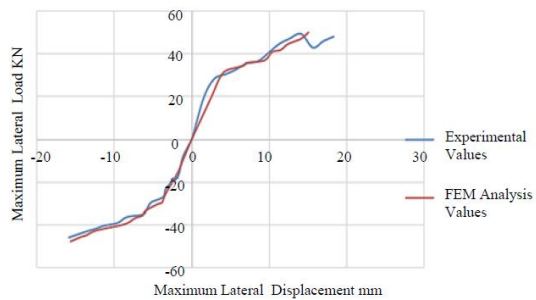
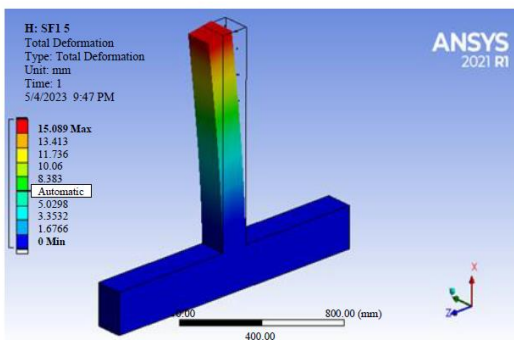




(d) Maximum displacement - SFBCJ 1



(e) Maximum displacement - SFBCJ 1.25



(f) Maximum displacement - SFBCJ 1.5

Fig. 6 (a), (b), (c), (d), (e), (f) Comparison of experimental values vs FEM analysis values

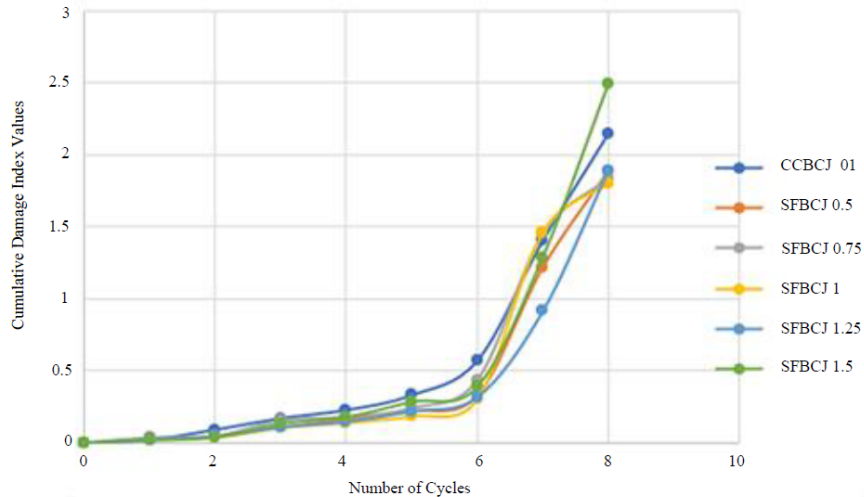


Fig. 7 Cumulative damage index vs number of cycles

Table 1. Input concrete properties

Sl. No	Specimen ID	Compressive Strength at 28days N/mm ²	Young's Modulus Ec GPa	Poisson Ratio of concrete(ν)
1	CCBCJ	32.75	28.613	0.189
2	SFBCJ 0.5	34.15	29.219	0.190
3	SFBCJ 0.75	34.78	29.48	0.191
4	SFBCJ 1	35.17	29.65	0.191
5	SFBCJ 1.25	35.78	29.908	0.192
6	SFBCJ 1.5	33.10	28.76	0.192

Table 2. Comparison of experimental vs finite element analysis values at peak loads (PL)

S. No	Specimens	Experimental Value				Finite Element Analysis Value			
		Lateral PL in KN	Displacement at PL in mm	Lateral PL in KN	Displacement at PL in mm	Lateral PL in KN	Displacement at PL in mm	Lateral PL in KN	Displacement at PL in mm
		+ Ve	+Ve	-Ve	-Ve	+ Ve	+Ve	-Ve	-Ve
1	CCBCJ 01	38.6	9.5	28.6	7.91	42.6	12.12	34.32	11.10
2	SFBCJ 0.5	41.4	11.2	37.2	10.1	45.4	12.75	41.49	11.21
3	SFBCJ 0.75	48.02	13.3	40.04	11.07	52.6	14.76	44.4	12.4
4	SFBCJ 1	50.74	15.88	48.62	13.56	54.12	15.27	49.18	12.8
5	SFBCJ 1.25	51.85	17.58	49.09	12.96	57.4	15.78	52.6	13.8
6	SFBCJ 1.5	48.25	18.3	47.47	14.45	50.26	15.08	49.7	14.12



5. Conclusion

The current work included experimental and computational studies to evaluate the effectiveness of sisal fibre reinforcement in external beam-column junctions. The ultimate loads of all specimens containing fibres were greater than those of the control specimen. The specimen containing 1.25% sisal fibre exhibited the greatest peak load of 57.2 KN during the forward cycle. The specimen containing 1.25% sisal fibre exhibited the maximum stress during the reverse cycle, measuring 52.6 kilonewtons (KN). It had the greatest total peak load. The specimen containing sisal fibre exhibited a greater maximum load as a result of the effective distribution of fibres and the ability to prevent fracture propagation via crack bridging. The research and experiment shown that the addition of 1.25% sisal fibre to reinforced concrete at the junction enhances the ductility of RCC external beam-column joints. Based on the analytical analysis, the use of sisal fibre reinforcement increased the ultimate load-carrying capacity and ductility of the joints when subjected to both upward and downward loading conditions.

References

1. Hasaballa, M., & El-Salakawy, E. (2016). Shear capacity of exterior beam-column joints reinforced with GFRP bars and stirrups. *Journal of Composites for Construction*, 20(2).
2. Dharmesh, N., & Govindaraju, L. (2023). A study on shear frame structure by modal superposition method. *International Journal of Engineering Trends and Technology*, 71(2), 457-465.
3. Laseima, S. Y., et al. (2020). Seismic behavior of exterior RC beam-column joints retrofitted using CFRP sheets. *Latin American Journal of Solids and Structures*, 17, 124-129.
4. Le-Trung, K., et al. (2010). Experimental study of RC beam-column joints strengthened using CFRP composites. *Composites Part B: Engineering*, 41(1), 76-85.
5. Mukherjee, A., & Joshi, M. (2005). FRPC reinforced concrete beam-column joints under cyclic excitation. *Composite Structures*, 70(2), 185-199.
6. Chidambaram, R. S., & Agarwal, P. (2015). Seismic behavior of hybrid fiber reinforced cementitious composite beam-column joints. *Materials & Design*, 86, 771-781.
7. Okeola, A. A., Mwero, J., & Bello, A. (2021). Behavior of sisal fiber-reinforced concrete in exterior beam-column joint under monotonic loading. *Asian Journal of Civil Engineering*, 22, 627-636.
8. Realfonzo, R., Napoli, A., & Ruiz Pinilla, J. G. (2014). Cyclic behavior of RC beam-column joints strengthened with FRP systems. *Construction and Building Materials*, 54, 282-297.
9. Haricharan, S., & Ranga Reddy, R. S. (2020). Modeling and analysis of reinforced concrete beam without transverse reinforcement and strengthened with CFRP lamellas: A parametric study. *SSRG International Journal of Civil Engineering*, 7(7), 123-127.
10. Venkatesan, B., et al. (2016). Finite element analysis (FEA) for the beam-column joint subjected to cyclic loading was performed using ANSYS. *Circuits and Systems*, 7(8).
11. Ali, A. Y., & Al-Rammahi, A. A. (2019). Flexural behavior of hybrid-reinforced concrete exterior beam-column joints under static and cyclic loads. *Fibers*, 7(10).
12. Padmanabham, K., & Sai, L. J. (2022). Experimental study on RC exterior beam-column joint retrofitted by post installation technique. *SSRG International Journal of Civil Engineering*, 9(12), 7-20.
13. Lee, W. T., Chiou, Y. J., & Shih, M. H. (2010). Reinforced concrete beam-column joint strengthened with carbon fiber reinforced polymer. *Composite Structures*, 92(1), 48-60.
14. Truong, G. T., et al. (2017). Seismic performance of exterior RC beam-column joints retrofitted using various retrofit solutions. *International Journal of Concrete Structures and Materials*, 11, 415-433.



15. Dharmesh, N., & Govindaraju, L. (2023). Sensitivity analysis of RC beam under flexure and shear by FOSM method. *International Journal of Engineering Trends and Technology*, 71(1), 141-151.
16. Shannag, M. J., Barakat, S., & Abdul-Kareem, M. (2002). Cyclic behavior of HPFRC-repaired reinforced concrete interior beam-column joints. *Materials and Structures*, 35, 348-356.
17. Bharathi, S. M. L., & Kumar, M. (2019). An experimental study on the flexural behaviour of natural fibre reinforced concrete with partial replacement of flyash and GGBS. *SSRG International Journal of Civil Engineering*, 6(4), 46-49.
18. Nallusamy, S., & Karthikeyan, A. (2017). Synthesis and wear characterization of reinforced glass fiber polymer composites with epoxy resin using granite powder. *Journal of Nano Research*, 49(1), 1-9.
19. Ganesan, N., Indira, P. V., & Sabeena, M. V. (2014). Behaviour of hybrid fibre reinforced concrete beam-column joints under reverse cyclic loads. *Materials & Design (1980-2015)*, 54, 686-693.
20. Faleschini, F., et al. (2017). Experimental behavior of beam-column joints made with EAF concrete under cyclic loading. *Engineering Structures*, 139, 81-95.
21. Erdem, R. T., et al. (2022). Impact analysis of a concrete beam via generative adversarial networks. *International Journal of Recent Engineering Science*, 9(1), 16-21.
22. Bagheri, H., & Mirzaie, K. (2023). Predicting the response of concrete columns to eccentric loading using finite element analysis. *SSRG International Journal of Civil Engineering*, 10(4), 1-7.
23. Abd Rahman, N., et al. (2022). Performance of modified foam concrete-filled column hollow sections. *International Journal of Engineering Trends and Technology*, 70(7), 399-404.
24. Bishetti, P., et al. (2019). Glass fiber reinforced concrete. *SSRG International Journal of Civil Engineering*, 6(6), 23-26.
25. Sivasankaran, U., Raman, S., & Nallusamy, S. (2019). Experimental analysis of mechanical properties on concrete with nano silica additive. *Journal of Nano Research*, 57, 93-104.
26. Abbadi, M. S., & Lamdouar, N. (2021). Seismic performance limit states assessment of bridge piers by numerical analysis and experimental damage observations. *International Journal of Engineering Trends and Technology*, 69(10), 168-177.
27. Park, Y.-J., et al. (1985). Seismic damage analysis of reinforced concrete buildings. *Journal of Structural Engineering*, 111(4), 740-757.